

Dominant recombination centers in Ga(In)NAs alloys: Ga interstitials

X. J. Wang,¹ Y. Puttisong,¹ C. W. Tu,² Aaron J. Ptak,³ V. K. Kalevich,⁴ A. Yu. Egorov,⁴ L. Geelhaar,^{5,a)} H. Riechert,^{5,a)} W. M. Chen,¹ and I. A. Buyanova^{1,b)}

¹Department of Physics, Chemistry, and Biology, Linköping University, S-581 83 Linköping, Sweden

²Department of Electrical and Computer Engineering, University of California, La Jolla, California 92093, USA

³National Renewable Energy Laboratory, Golden, Colorado 80401, USA

⁴A. F. Ioffe Physico-Technical Institute, St. Petersburg 194021, Russia

⁵Paul-Drude-Institut für Festkörperelektronik, 10117 Berlin, Germany

(Received 15 September 2009; accepted 25 November 2009; published online 16 December 2009)

Optically detected magnetic resonance measurements are carried out to study formation of Ga interstitial-related defects in Ga(In)NAs alloys. The defects, which are among dominant nonradiative recombination centers that control carrier lifetime in Ga(In)NAs, are unambiguously proven to be common grown-in defects in these alloys independent of the employed growth methods. The defects formation is suggested to become thermodynamically favorable because of the presence of nitrogen, possibly due to local strain compensation. © 2009 American Institute of Physics. [doi:10.1063/1.3275703]

Ga(In)As_{1-x}N_x alloys with low N content have recently sparked a considerable interest because of their unusual physical properties and their potential device applications.¹ When a small fraction of As atoms in Ga(In)As is replaced by N, the energy gap of the material decreases by as much as 150 meV per N mole fraction (the so-called giant bowing effect)² whereas its lattice shrinks. This makes this material promising for long wavelength telecommunications lasers on a GaAs substrate and highly efficient hybrid solar cells. Up to now, however, a major obstacle for full exploration of these devices is degradation of radiative efficiency and carrier mobility of Ga(In)NAs when N content increases, mainly due to severe nonradiative recombination (NRR) defects and carrier-scattering centers. Many theoretical and experimental efforts were devoted to identifying the NRR centers, however, their origin is still being debated.^{3–11}

Most recently, we have shown¹² that harmful NRR defects in Ga(In)NAs can be turned into an advantage, making this material a very efficient spin filter capable of generating more than 35% electron spin polarization at room temperature (RT) and without applied magnetic field via spin-dependent recombination (SDR). SDR requires presence of deep paramagnetic centers^{13–15} and relies on the Pauli's exclusion principle, which forbids capture of spin-polarized free electrons by NRR centers with the same spin orientation of localized electrons—see the insets in Fig. 1. Consistently, an enhancement of photoluminescence (PL) intensity of band-to-band (BB) recombination can be observed when competing recombination via the SDR centers is spin blocked due to spin polarization of free and localized carriers, e.g., under circularly polarized optical excitation.^{15,16} An example of such spin blockade is demonstrated in Fig. 1 which shows RT PL spectra due to the BB transitions from a GaNAs epilayer measured under circularly (σ) and linearly (π) polarized optical excitations, i.e., under conditions when the competing NRR via the deep centers is turned off and on, respectively. A dramatic (up to 8 times!) increase in the PL

intensity is observed under spin blockade, i.e., up to 88% of recombination suffers nonradiative losses via NRR under conventional conditions without spin polarization. The dominant NRR centers responsible for this SDR effect in GaNAs grown by gas source molecular beam epitaxy (GS-MBE) were unambiguously identified as Ga_i self-interstitial defects,¹² with a large capture rate of free electrons, e.g., up to 15 ps⁻¹ at RT for the GaN_{0.012}As_{0.988} multiple quantum wells (QW) grown at 420 °C.¹² An essential question arises whether these important NRR centers commonly form in Ga(In)NAs alloys, which is addressed in detail here by employing optically detected magnetic resonance (ODMR) technique. This technique is capable of singling out, among many defects present in a semiconductor material, only those which participate in recombination processes.¹⁷

We studied more than 30 undoped Ga(In)NAs epilayers and QW structures grown by common epitaxial techniques,

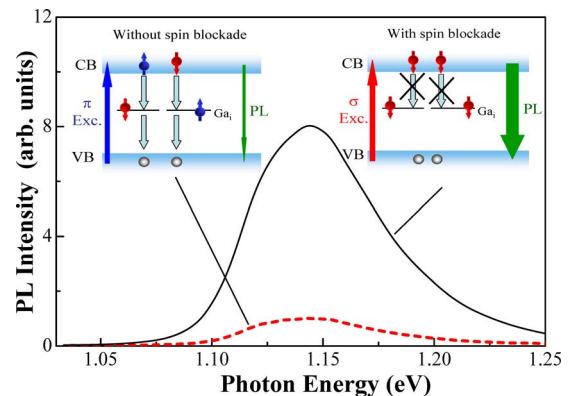


FIG. 1. (Color online) PL spectra of the BB emission measured under circular (solid line) and linear (dashed line) excitation from the GS MBE-grown GaN_{0.021}As_{0.979} epilayer subjected to *in situ* thermal anneal. The excitation photon energy was 1.312 eV. The insets schematically illustrate SDR via a NRR Ga_i interstitial defect in GaNAs. When both free and localized electrons are spin polarized under circularly (σ) polarized photoexcitation, NRR via the defects is spin blocked. This results in a stronger intensity of the BB PL as compared with that under linear (π) polarized excitation when the spin blockade is lifted and photoexcited carriers mainly recombine via the NRR centers.

^{a)}Formerly at Infineon Technologies, 81730 Munich, Germany.

^{b)}Electronic mail: irb@ifm.liu.se.

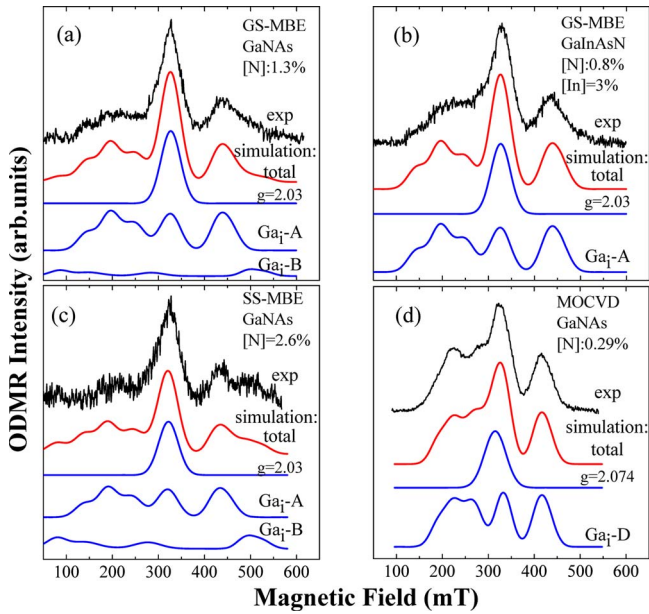


FIG. 2. (Color online) Representative ODMR spectra measured from as-grown Ga(In)NAs epilayers produced by the specified epitaxial techniques. The upper-most curves in (a)–(d) represent experimental spectra by monitoring the total intensity of the BB PL emission. Simulated ODMR spectra of the identified defects are also shown by the lower curves.

including GS-MBE, solid-source MBE (SS-MBE) and metal-organic chemical vapor deposition (MOCVD). The GS-MBE GaNAs epilayers and QWs have N compositions $[N]=0.7\text{--}3.3\%$ and were grown at temperatures $T_g=420\text{--}450\text{ }^\circ\text{C}$. Some of the samples were annealed either *in situ* at $700\text{ }^\circ\text{C}$ for 3 min or *ex situ* utilizing rapid thermal annealing (RTA) at $850\text{ }^\circ\text{C}$ for 10 s with a halogen lamp in N_2 ambient. A lower $T_g=390\text{ }^\circ\text{C}$ was employed during the SS-MBE growth of a $\text{GaN}_{0.026}\text{As}_{0.974}$ epilayer. During the GS- and SS-MBE growths, N was incorporated from a rf plasma source. The MOCVD growth was conducted at $550\text{--}600\text{ }^\circ\text{C}$ using dimethylhydrazine as a precursor for N. N composition in the MOCVD-grown alloys varied between 0.3% and 1%. Thicknesses of the GaNAs epilayers were $0.1\text{--}0.11\text{ }\mu\text{m}$ (GS-MBE), $0.1\text{ }\mu\text{m}$ (SS-MBE), and $1\text{ }\mu\text{m}$ (MOCVD). To evaluate effects of In incorporation on defect formation, $0.5\text{ }\mu\text{m}$ thick GS-MBE $\text{Ga}_{0.97}\text{In}_{0.03}\text{N}_{0.008}\text{As}_{0.992}$ and $1\text{ }\mu\text{m}$ thick MOCVD $\text{Ga}_{0.92}\text{In}_{0.08}\text{N}_{0.025}\text{As}_{0.975}$ epilayers were also studied. PL measurements were performed at RT, excited by circularly and linearly polarized light from a Ti:sapphire laser at a wavelength of $840\text{--}855\text{ nm}$. The excitation light propagated along the growth direction and the resulting PL was measured in a back-scattering geometry. ODMR experiments were done at 2.5 K and $\sim 9.3\text{ GHz}$. PL was excited by a Ti:sapphire laser at a wavelength of 850 nm . The excitation light was circularly polarized, to enhance the ODMR intensity.¹² ODMR signals were detected as spin resonance induced changes of PL intensity monitored by a Ge detector with proper optical filters.

Figure 2 summarizes results from the ODMR measurements and shows representative ODMR spectra from the GaNAs alloys grown by GS-MBE (a), SS-MBE (c), and MOCVD (d). Similar ODMR spectra were obtained by monitoring the BB PL and defect-related emissions at lower energies. The observed ODMR signals correspond to a decrease in the PL intensity of all emissions upon spin-resonant

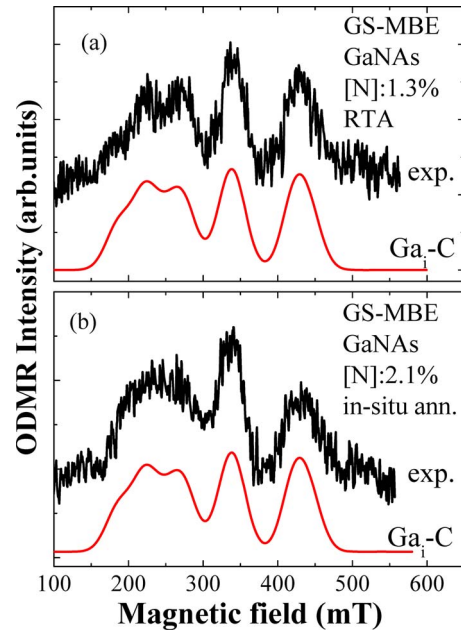


FIG. 3. (Color online) Experimental and simulated ODMR spectra measured from the GS-MBE grown epilayers subjected to post growth annealing either by using RTA (a) or *in situ* (b). The ODMR spectrum shown in (a) was measured from the same sample as shown in Fig. 2(a) but after RTA. The ODMR spectrum shown in (b) was measured from the same $\text{GaN}_{0.021}\text{As}_{0.979}$ epilayer as used to illustrate the SDR effect in Fig. 1(b).

transitions. This unambiguously proves that the corresponding defects act as efficient NRR centers, competing with the monitored radiative recombination processes. A careful analysis of the spectra revealed that they contain several components originating from different defects. The first component is a single line situated in the middle of the ODMR spectra with a g -value close to 2. Positive identification of the corresponding defect is not possible, unfortunately, due to lack of a resolved hyperfine (HF) structure. This defect is probably due to intrinsic defects or residual contaminants (e.g., O and C) with zero or weak HF interaction. It appeared under certain growth conditions as it was only found in some of the samples. It can be efficiently removed by RTA, see Fig. 3(a) that shows an ODMR spectrum of the same sample as that in Fig. 2(a) but after RTA. Other components in the ODMR spectra can be attributed to complex defects which contain an interstitial Ga_i atom in the core.¹² Indeed, the corresponding multiline, isotropic ODMR spectra can be described by the spin Hamiltonian $H = \mu_B g \mathbf{B} \cdot \mathbf{S} + \mathbf{A} \cdot \mathbf{S} \cdot \mathbf{I}$. Here μ_B is the Bohr magneton, \mathbf{B} is an external magnetic field, g denotes an electron g -factor, and A is a central HF interaction constant. The effective electron spin is $S=1/2$ and the nuclear spin is $I=3/2$. The spin Hamiltonian parameters for Ga_i -related defects, which were obtained from the best fit to the data, are summarized in Table I.

Very good agreement between the experimental ODMR spectra and results of simulations using the spin Hamiltonian was obtained for all samples, justifying the suggested defect origin. Four types of Ga interstitial-containing defects denoted as $\text{Ga}_i\text{-A}$, $\text{Ga}_i\text{-B}$, $\text{Ga}_i\text{-C}$, and $\text{Ga}_i\text{-D}$ were found, which differ in their strengths of the HF interaction—see Fig. 2 and also Table I. The same defects were also present in the GS-MBE and MOCVD grown GaInNAs alloys (at least for the studied In compositions $\leq 8\%$) as demonstrated in Fig. 2(b) taking as an example the GS-MBE $\text{Ga}_{0.97}\text{In}_{0.03}\text{N}_{0.008}\text{As}_{0.992}$

TABLE I. Spin Hamiltonian parameters determined from a best fitting of the spin Hamiltonian to the experimental ODMR data for the Ga_i-related defects in Ga(In)NAs. The ratio $A(^{71}\text{Ga})/A(^{69}\text{Ga})$ was deduced as 1.27–1.3, i.e., close to that of their nuclear magnetic moments $\mu(^{71}\text{Ga})/\mu(^{69}\text{Ga})=1.27$.

	Ga _i -A	Ga _i -B	Ga _i -C	Ga _i -D
g	2.035	2.000	2.000	2.010
$A(^{69}\text{Ga}_i), 10^{-4} \times \text{cm}^{-1}$	745	1230	620	580
$A(^{71}\text{Ga}_i), (10^{-4} \times \text{cm}^{-1})$	968.5	1562	787.4	736.6

epilayer. Intensities of the Ga_i-related ODMR signals, integrated over the multiline spectra, are higher than that for the “ $g=2$ ” line, underlining their more important role in NRR.

The observed differences in the values of the HF interaction for the Ga_i-related defects indicate a varying degree of localization of the electron wave functions at the core Ga_i atom. The likely reason is their different local surrounding (e.g., neighboring atoms within a complex defect containing Ga_i) as well as geometric locations, since three different self-interstitial sites are available in a zinc-blende lattice. It is interesting to note that the preferable local configurations of the formed defects seem to depend on growth conditions. Indeed Ga_i-A and Ga_i-B prevail in the MBE alloys grown at low temperatures [Figs. 2(a)–2(c)]. The defects, however, can be either partially annealed out or transformed into the Ga_i-C configuration by thermal annealing at 700–850 °C—see Fig. 3. This may indicate that Ga_i-C is more thermodynamically preferable. On the other hand, the Ga_i-D defect was only found in the MOCVD-grown Ga(In)NAs [Fig. 2(d)], possibly due to differences in growth conditions (e.g., higher $T_g=550$ – 600 °C and processes leading to layer growth) as well as in residual contamination.

No matter in what exact configurations the Ga interstitial defects form, however, the most important conclusion from our study is that the defects are abundant in all structures, independent of the employed growth methods—Fig. 2. This unambiguously proves that these highly efficient NRR centers are common grown-in defects in Ga(In)NAs alloys. Moreover, the defects are highly stable and cannot be fully removed by thermal annealing. Hence, identifying growth conditions that suppress their formation is crucial for device applications. We would also like to point out that the formation of Ga interstitials was also reported for Ga(Al,In)NP alloys,^{18,19} i.e., it is a common process in all dilute nitrides. A very important question, therefore, is how the Ga_i complex defects are formed. These defects have never been observed in N-free GaAs epilayers under similar growth conditions, which implies that their formation is related to introduction of N. On the other hand, we do not have evidence for a direct involvement of a N atom as a partner with Ga_i, neither substitutional nor interstitial,^{3–5} as no HF interaction from N has been resolved in spite of its nuclear spin $I=1$. Recently, we have shown that formation of Ga interstitials in GaNP is largely assisted by bombardment of N ions during the MBE growth process.²⁰ In principle, this could explain the defect formation in all Ga(In)NAs structures grown by MBE with a rf plasma N source. However, Ga_i are also present in the MOCVD-grown alloys where such bombardment is absent.

Therefore, the ion bombardment could not be the sole reason for the defect formation. It should be facilitated by the presence of N itself and should be thermodynamically favorable. Even though the exact physical mechanism behind the defect formation is currently unknown, which requires in-depth future theoretical studies, we speculate that the presence of a Ga_i atom may be favorable to compensate a large lattice distortion in the vicinity of a N atom with a small atomic radius and, therefore, to minimize total strain energy of the alloy.

In conclusion, we have provided unambiguous experimental evidence that the defects involving Ga_i are the common grown-in defects in Ga(In)NAs alloys regardless of the growth methods employed for material fabrication. They act as efficient NRR centers which control carrier lifetime and degrade optical quality of the alloys. The defects formation is concluded to become thermodynamically favorable under the presence of N, possibly because of local strain compensation.

Financial support from the Swedish Research Council (VR) and Swedish Energy Agency is greatly appreciated. V.K.K. and A.Y.E. acknowledge financial support from the RAS. We are grateful to John Geisz and Sarah Kurtz for designing the MOCVD-grown samples.

- ¹For a review on GaNAs, see e.g., I. A. Buyanova and W. M. Chen, *Physics and Applications of Dilute Nitrides* (Taylor and Francis, New York, 2004).
- ²M. Weyers, M. Sato, and H. Ando, *Jpn. J. Appl. Phys., Part 2* **31**, L853 (1992).
- ³S. B. Zhang and S.-H. Wei, *Phys. Rev. Lett.* **86**, 1789 (2001).
- ⁴S. G. Spruytte, C. W. Colden, J. S. Harris, W. Wampler, P. Krispin, K. Ploog, and M. C. Larson, *J. Appl. Phys.* **89**, 4401 (2001).
- ⁵T. Ahlgren, E. Vainonen-Ahlgren, J. Likonen, W. Li, and M. Pessa, *Appl. Phys. Lett.* **80**, 2314 (2002).
- ⁶P. Krispin, V. Gambin, J. S. Harris, and K. H. Ploog, *J. Appl. Phys.* **93**, 6095 (2003).
- ⁷W. Li, M. Pessa, T. Ahlgren, and J. Decker, *Appl. Phys. Lett.* **79**, 1094 (2001).
- ⁸S. B. Zhang and S. H. Wei, *Phys. Rev. Lett.* **86**, 1789 (2001).
- ⁹N. Q. Thinh, I. A. Buyanova, P. N. Hai, W. M. Chen, H. P. Xin, and C. W. Tu, *Phys. Rev. B* **63**, 033203 (2001).
- ¹⁰I. P. Vorona, T. Mchedlidze, D. Dagnelund, I. A. Buyanova, W. M. Chen, and K. Köhler, *Phys. Rev. B* **73**, 125204 (2006).
- ¹¹J. Toivonen, T. Hakkarainen, M. Sopanen, H. Lipsanen, J. Oila, and K. Saarinen, *Appl. Phys. Lett.* **82**, 40 (2003).
- ¹²X. J. Wang, I. A. Buyanova, F. Zhao, D. Lagarde, A. Balocchi, X. Marie, C. W. Tu, J. C. Harmand, and W. M. Chen, *Nature Mater.* **8**, 198 (2009).
- ¹³C. Weisbuch and G. Lampel, *Solid State Commun.* **14**, 141 (1974).
- ¹⁴D. Paget, *Phys. Rev. B* **30**, 931 (1984).
- ¹⁵V. K. Kalevich, E. L. Ivchenko, M. M. Afanasiev, A. Yu. Shiryaev, A. Yu. Egorov, V. M. Ustinov, B. Pal, and Y. Masumoto, *JETP Lett.* **82**, 455 (2005).
- ¹⁶D. Lagarde, L. Lombez, X. Marie, A. Balocchi, T. Amand, V. K. Kalevich, A. Shiryaev, E. Ivchenko, and A. Egorov, *Phys. Status Solidi A* **204**, 208 (2007).
- ¹⁷W. M. Chen, *Thin Solid Films* **364**, 45 (2000).
- ¹⁸N. Q. Thinh, I. P. Vorona, I. A. Buyanova, W. M. Chen, S. Limpijumng, S. B. Zhang, Y. G. Hong, H. P. Xin, C. W. Tu, A. Utsumi, Y. Furukawa, S. Moon, A. Wakahara, and H. Yonezu, *Phys. Rev. B* **71**, 125209 (2005).
- ¹⁹I. P. Vorona, T. Mchedlidze, M. Izadifard, I. A. Buyanova, W. M. Chen, Y. G. Hong, H. P. Xin, and C. W. Tu, *Appl. Phys. Lett.* **86**, 222110 (2005).
- ²⁰D. Dagnelund, I. A. Buyanova, T. Mchedlidze, W. M. Chen, A. Utsumi, Y. Furukawa, S. Moon, A. Wakahara, and H. Yonezu, *Appl. Phys. Lett.* **88**, 101904 (2006).